

## Extraction of 2-Phenylethanol (PEA) from Aqueous Solution Using Ionic Liquids: Synthesis, Phase Equilibrium Investigation, Selectivity in Separation and Thermodynamic Models

Urszula Maria Domanska, Patrycja Okuniewska, Kamil Padaszyński,  
Marta Królikowska, Maciej Zawadzki, and Mikolaj Wieckowski

*J. Phys. Chem. B*, **Just Accepted Manuscript** • DOI: 10.1021/acs.jpcc.7b04294 • Publication Date (Web): 19 Jul 2017

Downloaded from <http://pubs.acs.org> on July 21, 2017

### Just Accepted

“Just Accepted” manuscripts have been peer-reviewed and accepted for publication. They are posted online prior to technical editing, formatting for publication and author proofing. The American Chemical Society provides “Just Accepted” as a free service to the research community to expedite the dissemination of scientific material as soon as possible after acceptance. “Just Accepted” manuscripts appear in full in PDF format accompanied by an HTML abstract. “Just Accepted” manuscripts have been fully peer reviewed, but should not be considered the official version of record. They are accessible to all readers and citable by the Digital Object Identifier (DOI®). “Just Accepted” is an optional service offered to authors. Therefore, the “Just Accepted” Web site may not include all articles that will be published in the journal. After a manuscript is technically edited and formatted, it will be removed from the “Just Accepted” Web site and published as an ASAP article. Note that technical editing may introduce minor changes to the manuscript text and/or graphics which could affect content, and all legal disclaimers and ethical guidelines that apply to the journal pertain. ACS cannot be held responsible for errors or consequences arising from the use of information contained in these “Just Accepted” manuscripts.

1  
2  
3 **J. Phys. Chem. B**  
4

5  
6 **Extraction of 2-Phenylethanol (PEA) from Aqueous Solution Using Ionic**  
7  
8  
9 **Liquids: Synthesis, Phase Equilibrium Investigation, Selectivity in**  
10  
11  
12 **Separation and Thermodynamic Models**  
13

14  
15 Urszula Domańska,<sup>†‡\*</sup> Patrycja Okuniewska,<sup>†</sup> Kamil Padaszyński,<sup>†</sup> Marta Królikowska<sup>†</sup>  
16  
17 Maciej Zawadzki,<sup>†</sup> and Mikołaj Więckowski<sup>†</sup>  
18  
19

20  
21 Received: 6 May 2017  
22  
23  
24  
25  
26

27 <sup>†</sup> Prof. Dr. hab. U. Domańska, Msc. Eng. P. Okuniewska, Dr. Eng. K. Padaszyński, Dr. Eng.  
28  
29 M. Królikowska, Dr. Eng. M. Zawadzki, student M. Więckowski, Department of Physical  
30  
31 Chemistry, Faculty of Chemistry, Warsaw University of Technology, Noakowskiego 3, 00-  
32  
33 664 Warsaw (Poland).  
34  
35

36  
37 <sup>‡</sup> Prof. Dr. hab. U. Domańska, Thermodynamic Research Unit, School of Engineering,  
38  
39 University of KwaZulu-Natal, Howard College Campus, King George V Avenue, Durban  
40  
41  
42 4041 (South Africa)  
43  
44  
45  
46  
47  
48  
49  
50  
51  
52  
53  
54  
55  
56  
57  
58  
59  
60

**Abstract:** This study assessed the effect of ionic liquids (ILs) on extraction of 2-phenylethanol (PEA) from aqueous phase. It consists the synthesis of four new ILs, their physico-chemical properties and experimental solubility measurements in water as well as liquid-liquid phase equilibrium in ternary systems. ILs are an important new media for imaging and sensing applications because of their solvation property, thermal stability and negligible vapor pressure. However, complex procedures and non-miscibility with water are often required in PEA extraction. Herein, a facile and general strategy using four ILs as extraction media including the synthesis of new bis(fluorosulfonyl)imide-based ILs: 1-hexylmethylmorpholinium bis(fluorosulfonyl)imide, [HMMOR][FSI], *N*-octylisoquinolinium bis(fluorosulfonyl)imide, [OiQuin][FSI], 1-butyl-1-methylpyrrolidinium bis(fluorosulfonyl)imide, [BMPYR][FSI] and *N*-triethyl-*N*-octylammonium bis(fluorosulfonyl)imide, [N<sub>2228</sub>][FSI] were investigated. The thermal properties, density, viscosity and surface tension of new ILs were measured. Calorimetric measurements (DSC) were used to determine the melting point and the enthalpy of melting as well as the glass transition temperature and heat capacity at glass transition of the ILs. The phase equilibrium in binary systems (IL + PEA, or water) and in ternary systems {IL (1) + PEA (2) + water (3)} at temperature  $T = 308.15$  K and ambient pressure are reported. All systems presents liquid-liquid equilibrium with the Upper Critical Solution Temperature (UCST). All ILs revealed complete miscibility with PEA. In all ternary systems immiscibility gap was observed, which classified measured systems as Treybal's type II. The two partially miscible binaries (IL + water) and (PEA + water) exists in these systems. The discussion contains the specific selectivity and the solute distribution ratio of separation for the used ILs. The commonly used NRTL model was used for the correlation of the experimental binary and ternary systems with acceptable root mean square deviation. The prediction of binary and ternary compositions was provided with acceptable deviations using COSMO RS. The data of ternary LLE show the

1  
2  
3 possible use of [HMMOR][FSI] as a good entrainer for the separation of PEA from water  
4  
5 using solvent extraction.  
6  
7  
8  
9  
10  
11  
12  
13  
14  
15  
16  
17  
18  
19  
20  
21  
22  
23  
24  
25  
26  
27  
28  
29  
30  
31  
32  
33  
34  
35  
36  
37  
38  
39  
40  
41  
42  
43  
44  
45  
46  
47  
48  
49  
50  
51  
52  
53  
54  
55  
56  
57  
58  
59  
60

## ■ INTRODUCTION

2-Phenylethanol (PEA) is a valuable fragrance raw material of a rose flavour popular in perfume and household chemical industries.<sup>1-4</sup> PEA is used as well in food industry. According to new US Food and Drug Administration and European legislations the biotechnological method of production is suggested. It is the bioconversion of *L*-phenylalanine to PEA with *Saccharomyces cerevisiae* yeast in aqueous phase. The “*in situ*” product recovery is necessary in this process.<sup>4-6</sup> The selection of the suitable solvent including ILs has attracted the attention of a growing number of publications.<sup>1-6</sup> The possible other methods suggested to this process is absorption process on polymer for selective PEA removal,<sup>7</sup> or separation on membrane immersed in the bioreactor.<sup>8</sup>

Green technology requires new solvents as ILs to replace common volatile and toxic organic solvents. ILs are known as a class of tailoring solvents with high solvation properties and large selectivities in many separation processes.<sup>9</sup> However, the “green” character of ILs may be discussed only as for substances with very low vapour pressure. Unfortunately, many of ILs are toxic against fungi and bacteria and they reveal poor biodegradability, biocompatibility and sustainability.<sup>10</sup> ILs were suggested in literature for the separation of aromatic hydrocarbons from aliphatic hydrocarbons, sulfur compounds from aliphatic hydrocarbons, alkanes from alkenes, separation of azeotropic mixtures and many others.<sup>11-14</sup> Hydrophobic ILs are proposed very often as entrainers in liquid-liquid extraction.<sup>15</sup> ILs have been proposed to extract PEA from the aqueous phase after bio-synthesis as well.<sup>16-22</sup> The ILs used in the PEA extraction process must reveal large or complete miscibility with PEA and cannot be toxic to the yeast.<sup>16</sup>

A model experiment for the extraction in real biosynthesis is the liquid-liquid phase equilibrium (LLE) in ternary systems {IL + PEA + water}. In our laboratory, we have

1  
2  
3 undertaken various studies on factors influencing the extraction of PEA. We tested in ternary  
4 LLE many imidazolium-based, quinolinium-based, pyrrolidinium-based, ammonium-based,  
5 morpholinium-based and sulfonium-based ILs with bis{(trifluoromethyl)sulfonyl}imide  
6 anion.<sup>18-21</sup> We also investigated a series of tetracyanoborate-based ILs.<sup>22</sup> Recently, the Deep  
7 Eutectic Solvents (DES composed of (1-butyl-1-methylpyrrolidinium  
8 bis{(trifluoromethyl)sulfonyl}imide, [BMPYR][NTf<sub>2</sub>] + 2-methyl-2-butanol) and (1-hexyl-  
9 1-methylpyrrolidinium bis{(trifluoromethyl)sulfonyl}imide, [HMPYR][NTf<sub>2</sub>] + 2-methyl-2-  
10 butanol) were tested by us in this process.<sup>23</sup> Different solute distribution ratios ( $\beta_2$ ) and  
11 selectivities ( $S_{23}$ ) were observed in these ternary systems.

12  
13  
14  
15  
16  
17  
18  
19  
20  
21  
22  
23 In this study, we propose to extend the extraction measurements to the LLE ternary phase  
24 equilibria with new, synthesised by us bis(fluorosulfonyl)imide-based ILs with different  
25 cations.

26  
27  
28  
29  
30 The hydrophobic ILs consisting of bis(fluorosulfonyl)imide (FSI<sup>-</sup>) anion show  
31 promise as electrolytes for Li-ion-based electric storage devices, as they exhibit relatively low  
32 viscosity, high conductivity, wide electrochemical stability window and high chemical  
33 stability.<sup>24</sup> These ILs have been reported to inhibit dendrite formation on lithium metal and  
34 lithiated graphite electrodes, which was proved via matrix isolation electron paramagnetic  
35 resonance.<sup>24</sup> Among ILs, those composed of the [FSI]<sup>-</sup> anion are attracting attention, because  
36 the viscosity of imidazolium-based, or pyrrolidinium-based bis(fluorosulfonyl)imides are  
37 much lower than that of the respective bis{(trifluoromethyl)sulfonyl}imide, [NTf<sub>2</sub>].<sup>25</sup> Liquid  
38 structure studied by a high-energy *X*-ray scattering technique indicates that these ILs involves  
39 an ordered structure with significant intermolecular interactions at around 6, 10 and 16 Å.<sup>25</sup>  
40 The 1-ethyl-3-methylimidazolium bis(fluorosulfonyl)imide, ([EMIM][FSI]) has been studied  
41 by Raman spectra and theoretical DFT calculations. Three strong Raman bands were found  
42 for [EMIM][FSI] at 293, 328, and 360 cm<sup>-1</sup>, which are ascribed to the [FSI]<sup>-</sup> ion. This was  
43  
44  
45  
46  
47  
48  
49  
50  
51  
52  
53  
54  
55  
56  
57  
58  
59  
60

1  
2  
3 supported by theoretical calculations that the [FSI]<sup>-</sup> ion is present as either C<sub>2</sub> (trans) or C<sub>1</sub>  
4 (cis) conformer.<sup>26</sup> The physical and electrochemical properties of the mixture of Na[NTf<sub>2</sub>]  
5 with 1-propyl-1-methylpyrrolidinium bis(fluorosulfonyl)imide, [PMPYR][FSI] have been  
6  
7 determined to show that they have a potential for the sodium battery electrolyte.<sup>27</sup>  
8  
9

10  
11  
12 In this work, the following new ILs are proposed for physico-chemical and phase  
13 equilibrium measurements: 1-hexyl-1-methylmorpholinium bis(fluorosulfonyl)imide,  
14 [HMMOR][FSI], *N*-octylisoquinolinium bis(fluorosulfonyl)imide, [OiQuin][FSI], 1-butyl-1-  
15 methylpyrrolidinium bis(fluorosulfonyl)imide, [BMPYR][FSI] and *N*-triethyl-*N*-  
16 octylammonium bis(fluorosulfonyl)imide, [N<sub>2228</sub>][FSI]. The structure of the cation is  
17 responsible for the solvation properties of the IL and its extraction potential, the new anion has  
18 influence on the mutual solubility (IL + water).  
19  
20  
21  
22  
23  
24  
25  
26  
27  
28  
29

## 30 ■ EXPERIMENTAL SECTION

31  
32  
33 **Synthesis of [FSI]-based ILs.** [HMMOR][FSI] ([N(SO<sub>2</sub>F)<sub>2</sub>]): To a solution of 21.83 g  
34 *N*-hexyl-*N*-methylmorpholinium bromide (0.0820 mol, synthesized) in 50 cm<sup>3</sup> water a  
35 solution of 18.29 g sodium bis(fluorosulfonyl)imide (0.0900 mol, Provisco CS 99%, 9.8%  
36 excess, used as received) in 50 cm<sup>3</sup> of water was added. Immediately a second heavier phase  
37 forms. Next 100 cm<sup>3</sup> of dichloromethane was added. Mixture was stirred at room temperature  
38 for 4h and phases were separated by draining. Then organic phase was extracted with 10 x 15  
39 cm<sup>3</sup> of water (removal of residual sodium bromide and excess of sodium  
40 bis(fluorosulfonyl)imide). Solvents were removed in rotary evaporator and product was  
41 further dried under vacuum at 353 K for 48h. Product was obtained as a 28.39 g of pale  
42 yellow liquid. Yield 94.5% (see Report S1 in the Supporting Information, SI).  
43  
44  
45  
46  
47  
48  
49  
50  
51  
52  
53

54  
55 [OiQuin][FSI] ([N(SO<sub>2</sub>F)<sub>2</sub>]): To a solution of 22.88 g *N*-octylisoquinolinium bromide  
56 (0.0710 mol, synthesized) in 50 cm<sup>3</sup> water a solution of 15.57 g sodium  
57  
58  
59  
60

1  
2  
3 bis(fluorosulfonyl)imide (0.0781 mol, Provisco CS 99%, 10.1% excess, used as received) in  
4  
5 50 cm<sup>3</sup> of water was added. Immediately a second heavier phase forms. The volume of 100  
6  
7 cm<sup>3</sup> of dichloromethane was added. Mixture was stirred at room temperature for 4h and  
8  
9 phases were separated by draining. Then organic phase was extracted with 10 x 15 cm<sup>3</sup> of  
10  
11 water (removal of residual sodium bromide and excess of sodium bis(fluorosulfonyl)imide).  
12  
13 Solvents were removed in rotary evaporator and product was further dried under vacuum at  
14  
15 353 K for 48h. Product was obtained as a 29.19 g of yellow liquid. Yield 97.3% (see Report  
16  
17 S2 in the SI).  
18  
19

20 [BMPYR][FSI]: The bromide salt, used for further reaction was prepared according to  
21  
22 well known procedure. To a solution of 18.47 g *N*-butyl-*N*-methylpyrrolidinium chloride  
23  
24 (0.1039 mol, synthesized) in 50 cm<sup>3</sup> water a solution of 23.27 g sodium  
25  
26 bis(fluorosulfonyl)imide (0.1146 mol, Provisco 99%, 10% excess, used as received) in 50 cm<sup>3</sup>  
27  
28 of water was added. Immediately a second heavier phase forms. The volume of 100 cm<sup>3</sup> of  
29  
30 dichloromethane was added. Mixture was stirred at room temperature for 4h and phases were  
31  
32 separated by draining. Then organic phase was extracted with 10 x 15 cm<sup>3</sup> of water (removal  
33  
34 of residual sodium chloride and excess of sodium bis(fluorosulfonyl)imide). Solvents were  
35  
36 removed in rotary evaporator and product was further dried under vacuum at 353 K for 48h.  
37  
38 Product was obtained as a 32.08 g of colourless liquid. Yield 95.8% (see Report S3 in the SI).  
39  
40  
41  
42

43 [N<sub>2228</sub>][FSI]: The bromide salt, needed for further reaction was prepared according to  
44  
45 well known procedure. Triethylamine 12.20 g (0.1206 mol, Sigma - Aldrich 99%) and 1-  
46  
47 bromooctane 25.24 g (0.1307 mol, Sigma - Aldrich 99%, 8.4% excess) were used; product  
48  
49 was crystallized from acetonitrile and washed with ethyl acetate. Yield 79.6% (28.26 g)  
50  
51 To a solution of 28.10 g triethyloctylammonium bromide (0.0955 mol, synthesized) in 50 cm<sup>3</sup>  
52  
53 water, a solution of 20.99 g sodium bis(fluorosulfonyl)imide (0.1031 mol, Provisco 99%, 8%  
54  
55 excess, used as received) in 50 cm<sup>3</sup> of water was added. Next, a second heavier phase forms.  
56  
57  
58  
59  
60

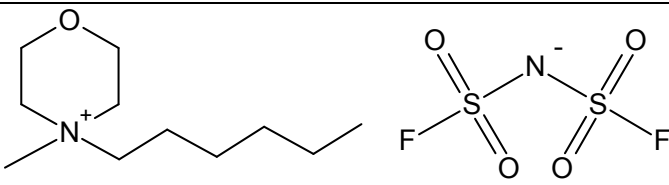
The volume of 100 cm<sup>3</sup> of dichloromethane was added. Mixture was stirred at room temperature for 4h and phases were separated by draining. Then organic phase was extracted with 10 x 15 cm<sup>3</sup> of water (removal of residual sodium bromide and excess of sodium bis(fluorosulfonyl)imide). Solvents were removed in rotary evaporator and product was further dried under vacuum at 413 K for 24h. Product was obtained as a 36.65 g of colourless liquid. Yield 97% (see Report S4 in the SI).

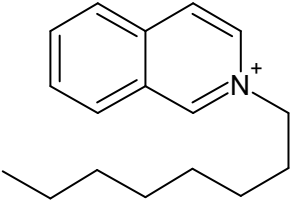
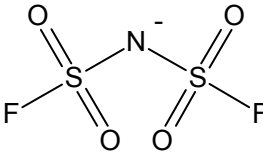
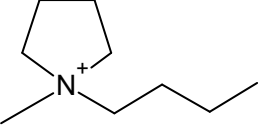
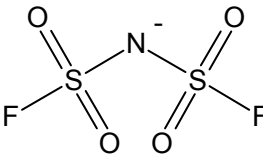
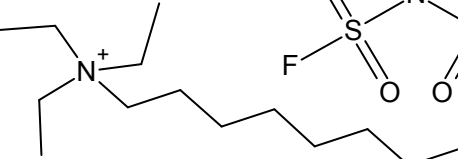
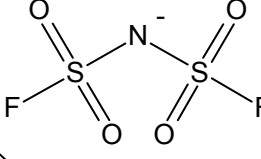
The purity of the ILs is shown in Reports S1-S5 in the SI. The structure, name, abbreviation of name, molar mass and water content of ILs used are listed in Table 1. All ILs were purified before use during 24 h under low pressure at  $T = 368$  K.

**Materials.** PEA (CAS: 60-12-8) was obtained from Merck. The freshly activated molecular sieves of type 4Å (Union Carbide) were used for drying PEA. Solubility of ILs was measured in doubly distilled and degassed water deionised by a Milipore purification system.

**Water content.** The Karl-Fischer titration technique (method TitroLine KF) was used for the analyzes of water. The sample of IL, or solvent was dissolved in methanol and titrated in steps of 0.0025 cm<sup>3</sup>. The uncertainty in the water content is  $\pm 10 \cdot 10^{-6}$  for the 3 cm<sup>3</sup> IL sample injected. The water content in ILs used is listed in Table 1.

**Table 1. Chemical Structures, Names, Abbreviations, Molar Mass and Water Content in Mass Fraction of the ILs Under Study**

Structure	Name, abbreviation	$M /$ (g·mol <sup>-1</sup> )	Water kontent weight fraction/ purity wt.
	1-hexyl-1-methylmorpholinium bis(fluorosulfonyl)imide, [HMMOR][FSI]	366.44	270x10 <sup>-6</sup> / 97.0%

		1-octylisoquinolinium bis(fluorosulfonyl)imide, [OiQuin][FSI]	422.51	311x10 <sup>-6</sup> 97.0%
		1-butyl-1-methylpyrrolidinium bis(fluorosulfonyl)imide, [BMPYR][FSI]	322.39	166x10 <sup>-6</sup> 97.4%
		Tri(ethyl)octylammonium bis(fluorosulfonyl)imide, [N <sub>2228</sub> ][FSI]	394.54	282x10 <sup>-6</sup> 97.5%

**Differential scanning microcalorimetry, DSC.** The temperatures of fusion ( $T_{\text{fus}}$ ), enthalpies of fusion ( $\Delta_{\text{fus}}H$ ), temperature of glass transition ( $T_{\text{g}}$ ), and heat capacity at glass transition ( $C_{p(\text{g})}$ ) have been measured using a differential scanning microcalorimetry technique (DSC) of new ILs. The applied scan rate was 5, or 2 K·min<sup>-1</sup>, with a power and recorder sensitivities of 16 mJ·s<sup>-1</sup> and 5 mV, respectively. The apparatus (Thermal Analysis Q200, USA with Liquid Nitrogen Cooling System) was calibrated with a 0.999999 mol fraction purity indium sample. The uncertainty of the melting temperature was  $u(T_{\text{fus}}) = \pm 0.1$  K (average over three scans). The uncertainty of the enthalpy of fusion was  $u(\Delta_{\text{fus}}H_1) = \pm 0.1$  kJ·mol<sup>-1</sup> and that of heat capacity at melting temperature  $u(\Delta C_{p,\text{g}}) = \pm 10$  J·mol<sup>-1</sup>·K<sup>-1</sup>. The new data are listed in Table 2. All DSC diagrams are shown in Figs. S1-S4 in the SI.

**Table 2. Thermophysical Properties of Pure ILs: Glass Transition Temperature ( $T_{\text{g}}$ ), Heat Capacity at Glass Transition Temperature ( $\Delta C_{p(\text{g})}$ ), Melting Temperature ( $T_{\text{fus}}$ ) and Enthalpy of Melting ( $\Delta_{\text{fus}}H$ ) Determined by DSC Technique<sup>a</sup>**

$T_{\text{g}} / (\text{K})$	$\Delta C_{p(\text{g})} / (\text{J}\cdot\text{mol}^{-1}\cdot\text{K}^{-1})$	$T_{\text{fus}} / (\text{K})$	$\Delta_{\text{fus}}H / (\text{kJ}\cdot\text{mol}^{-1})$
-----------------------------	---	-------------------------------	--

[HMMOR][FSI]	195.9	147		
[OiQuin][FSI]	204.7	156	303.3 (onset); 307.0 (peak)	27.2
[BMPYR][FSI]	167.7	119		
[N <sub>2228</sub> ][FSI]	180.2	158		

<sup>a</sup> Standard uncertainties  $u$  are as follows:  $u(T_{\text{fus}}) = \pm 0.1$  K,  $u(\Delta_{\text{fus}}H) = \pm 0.1$  kJ·mol<sup>-1</sup>,  $u(\Delta C_p) = 10$  J·mol<sup>-1</sup>·K<sup>-1</sup>.

**Density measurements.** The Anton Paar GmbH 4500 vibrating-tube densimeter (Graz, Austria), thermostated at different temperatures was used for the measurements of density. Two integrated Pt 100 platinum thermometers were used for the temperature control internally ( $T \pm 0.01$  K). Densimeter includes an automatic correction for the viscosity of the sample. The precision of the measurements is  $1 \cdot 10^{-5}$  g·cm<sup>-3</sup>, and the uncertainty of the measurements was assumed to be better than  $u(\rho) = \pm 1.4 \cdot 10^{-3}$  g·cm<sup>-3</sup> (including impurities). The densimeter's calibration was performed at atmospheric pressure using doubly distilled and degassed water (PURE LAB Option Q Elga Water System), specially purified benzene (CHEMIPAN, Poland 0.999) and dried air. The densities of the ILs are listed in Table S1 in the SI.

**Viscosity measurements.** Viscosity measurements for [N<sub>8,2,2,2</sub>][NTf<sub>2</sub>] and [N<sub>8,8,8,1</sub>][NTf<sub>2</sub>] were provided using an Anton Paar GmbH AMVn (Graz, Austria) programmable viscometer, with a nominal uncertainty of  $u(\eta) = \pm 0.5$  % for viscosities from 10 mPa·s to 390 mPa·s. Temperature was controlled internally with a precision of  $\pm 0.01$  K in a range from (298.15 to 368.15) K. The uncertainty was  $u(T) = \pm 0.1$  K. In the measured viscosity range the diameter of the capillary was 1.8 mm, 3.0 mm and 4.0 mm for the following viscosity range: (10 to 70) mPa·s, (20 to 230) mPa·s and (230-390) mPa·s, respectively. The experimental dynamic viscosity of pure ILs are listed in Table S1 in the SI.

**Surface tension measurements.** The surface tension measurements were made with a Tensiometer KSV Sigma 701 System (Finland) using a Du-Noüy ring taking into account the Zuidema Waters correction.<sup>28-30</sup> All measurements were repeated three to five times. The

1  
2  
3 uncertainty of the measurement is  $u(\sigma) = \pm 0.04 \text{ mN}\cdot\text{m}^{-1}$  and that of temperature is  $u(T) = \pm$   
4  
5 0.1 K. The experimental values of surface tension of pure ILs are listed in Table S1 in the SI.  
6  
7

8 **Procedure in binary systems.** The solubility of IL in PEA and water was measured  
9  
10 with dynamic (synthetic) method.<sup>18-23</sup> The sample was prepared by weighing with an  
11  
12 uncertainty of  $1 \times 10^{-4}$  g. The solid-liquid equilibrium was detected with an increasing  
13  
14 temperature ( $< 2 \text{ K}\cdot\text{h}^{-1}$ ) with continuous stirring inside a Pyrex glass cell placed in a  
15  
16 thermostat. Temperature was measured with an electronic thermometer P 750 (DOSTMANN  
17  
18 electronic GmbH) with an uncertainty to be  $u(T) = \pm 0.2 \text{ K}$ ,  $u(p) = \pm 0.1 \text{ kPa}$ . The uncertainty  
19  
20 in the mole fraction is  $u(x) = \pm 0.0005$ .  
21  
22  
23

24 The experimental solubility of the IL in water (liquid + liquid phase diagram in the  
25  
26 water-rich phase) for all ILs was determined with a conductivity method.<sup>20,31</sup> The conductivity  
27  
28 of the aqueous solution was measured using a Mettler Toledo FiveEasy FE 30, coupled with  
29  
30 an LE 703 Conductivity Probe as the electrode. The calibration curves were performed for  
31  
32 each IL in an adequate concentration range and containing the same amount of 2-propanol.  
33  
34 Solubility results, at each temperature, are the average of three measurements of individual  
35  
36 samples. Conductivity accuracy is  $\pm 0.5\%$ . The uncertainty of mole fraction was  $u(x) =$   
37  
38  $\pm 0.000001$ , temperature and pressure  $u(T) = \pm 0.1 \text{ K}$ ,  $u(p) = \pm 0.1 \text{ kPa}$ . All weighing involved  
39  
40 in the experimental work was carried out using a Mettler Toledo AB 204-S balance, with a  
41  
42 precision of  $\pm 1 \times 10^{-4}$  g.  
43  
44  
45  
46

47 **Procedure in ternary systems.** The LLE equilibrium experiment in four systems was  
48  
49 carried out in a jacketed vessel of volume  $10 \text{ cm}^3$ . The procedure is described in our previous  
50  
51 work.<sup>19-21</sup> Propan-1-ol was used as internal standard for the GC-analysis (PerkinElmer Clarus  
52  
53 580 GC equipped with auto sampler and FID and TCD detectors) of PEA and water. Details  
54  
55 of the operational conditions of the apparatus are reported in Table S2 in the SI. The estimated  
56  
57  
58  
59  
60

1  
2  
3 uncertainty in the determination of mole fraction compositions is  $u(x) = 0.003$ .  
4  
5

### 7 ■ Theory (Conductor-like screening model for real solvents)

8  
9  
10 Conductor-like screening model for real solvents (COSMO-RS) is a state of the art model  
11 combining principles of unimolecular quantum chemical (QC) calculations and statistical  
12 mechanics (SM).<sup>32-34</sup> The QC basis of COSMO-RS in conductor-like screening model (the  
13 “COSMO” part of the model), originally was proposed and developed by Klamt and  
14 Schüürmann.<sup>35</sup> The key property obtained from COSMO is the distribution of the density of  
15 screening charge induced at its surface by the surrounding conductor ( $\sigma$ ). The *ab initio*  
16 calculated  $\sigma$  require probability distribution (histogram) of  $\sigma$  at the cavity’s surface, denoted  
17 by  $p(\sigma)$  and called  $\sigma$ -profile. Given  $\sigma$ -profiles of all the components present in the mixture,  
18 their chemical potentials  $\mu$  can be calculated by using the following formula:  
19  
20  
21  
22  
23  
24  
25  
26  
27  
28  
29  
30  
31  
32

$$\mu_i = \mu_i^{\text{comb}} + \int p(\sigma) \mu_s(\sigma) d\sigma + RT \ln x_i \quad (1)$$

33  
34  
35  
36  
37  
38  
39  
40 where  $\mu_i^{\text{comb}}$  denotes combinatorial contribution due to differences in size and shape, whereas  
41  
42  $\mu_s(\sigma)$  stands for the chemical potential of the surface segment of screening charge density  $\sigma$ .  
43  
44

45 In this work, COSMO-RS model was applied to predict LLE phase behaviour of the  
46 binary and ternary systems under study. All the calculations were carried out using  
47 COSMOtherm suite (version 17.0.1; updated on February 2017) purchased from  
48 COSMOlogic GmbH & Co. KG (Leverkusen, Germany).<sup>36</sup> The COSMO files representing  $\sigma$   
49 and thus  $\sigma$ -profiles for each molecule considered (i.e. four cations, [FSI]<sup>-</sup> anion, PEA and  
50 water, see Table 1) were obtained by using Turbomole quantum chemical suite<sup>37</sup> purchased  
51  
52  
53  
54  
55  
56  
57  
58  
59  
60

1  
2  
3 from COSMOlogic as well. The standard COSMO cavities and the corresponding  $\sigma$ -profiles  
4  
5 used in the final calculations were obtained using the most common BP-TZVP-COSMO level  
6  
7 of density functional theory (DFT) utilized in COSMO-RS modeling,<sup>38,39</sup> and triple- $\zeta$  valence  
8  
9 polarized basis set.<sup>40</sup> Consequently, parameterization BP\_TZVP\_C30\_1701 of the COSMO-  
10  
11 RS was applied.  
12

13  
14 The calculated  $\sigma$  spatial distributions and the respective  $\sigma$ -profiles are given in Fig. 1.  
15  
16 As seen, all the cations display similar shape of the  $\sigma$ -profiles. In general, all of them cover  
17  
18 “non-polarity” range ( $-1 < \sigma / \text{e}\cdot\text{nm}^{-2} < 1$ ), while being shifted towards negative values of  $\sigma$ .  
19  
20 Due to the most considerable contribution of alkyl chains,  $[\text{N}_{2228}]^+$  cation discloses much  
21  
22 more screening charge in compared to the other cations. On the other hand, “bimodal-like”  $\sigma$ -  
23  
24 profile of  $[\text{FSI}]^-$  anion indicates that its cavity surface can be divided into two domains, one of  
25  
26 which is strongly basic (oxygen atoms of sulfonyl groups and nitrogen atom in the center of  
27  
28 the molecule), whereas the second is only slightly polar (terminal fluorine atoms). The  $\sigma$ -  
29  
30 profile of PEA displays small peaks in  $H$ -bond donor and acceptor range of  $\sigma$  ( $\sigma < -1 \text{ e}\cdot\text{nm}^{-2}$   
31  
32 and  $\sigma < +1 \text{ e}\cdot\text{nm}^{-2}$ , respectively) due to the presence of OH group and a wide peak in non-  
33  
34 polarity range due to alkyl chain. Obviously, in the case of water, the non-polar part of the  $\sigma$ -  
35  
36 profile is not observed – the molecule is amphoteric, with a little bit better capacity of acting  
37  
38 as donor in  $H$ -bonding formation.  
39  
40  
41  
42  
43  
44  
45  
46  
47  
48  
49  
50  
51  
52  
53  
54  
55  
56  
57  
58  
59  
60

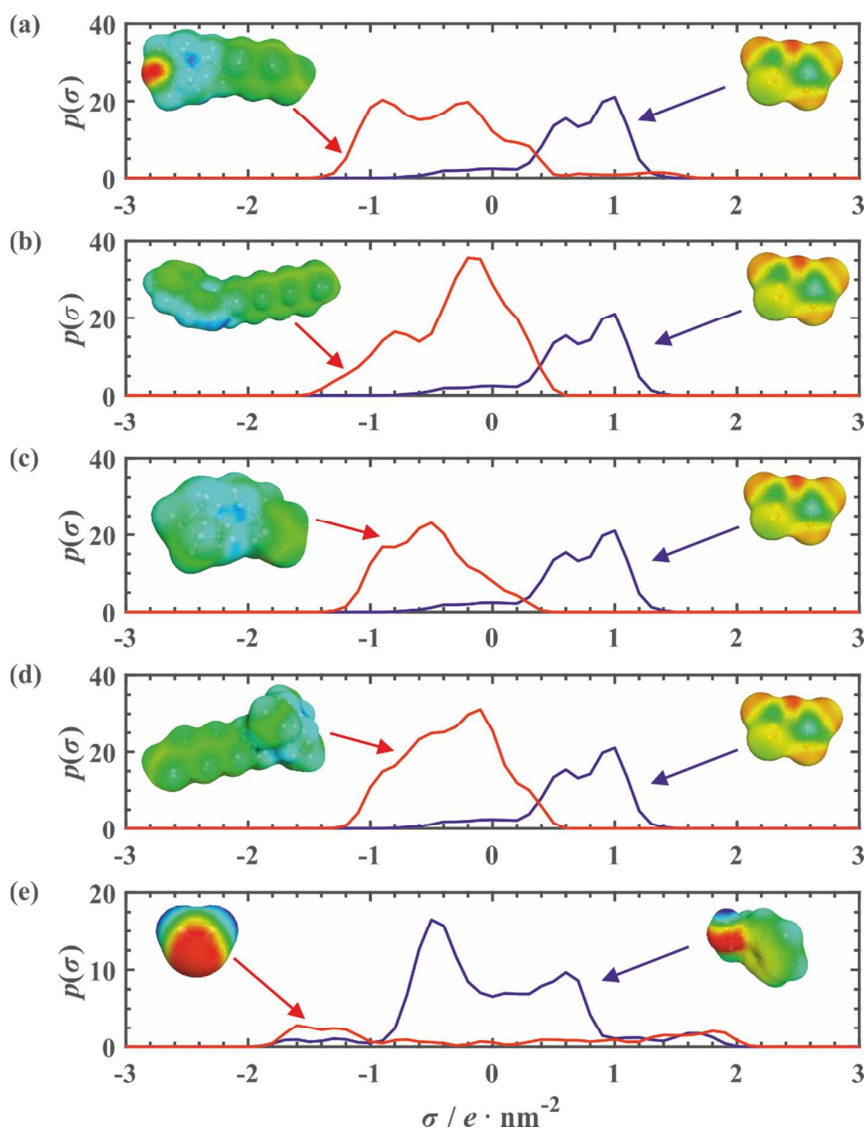


**Figure 1.** Screening charge density ( $\sigma$ ) of the ions forming ILs and molecular solvents (PEA and water) calculated at BP-TZVP-COSMO level along with the corresponding  $\sigma$ -profiles used in COSMO-RS predictions of LLE in ternary systems under study: (a) [HMMOR][FSI]; (b) [QiQuin][FSI]; (c) [BMPYR][FSI]; (d) [N<sub>2228</sub>][FSI]; (e) PEA (r.h.s.) and water (l.h.s.). In panels a–d, spatial  $\sigma$  distributions of cation and [FSI] anion are shown on the l.h.s. and r.h.s., respectively.

## ■ RESULTS AND DISCUSSION

**DSC results.** From the thermographs of ILs it can be noted that only [OiQuin][FSI] exhibits temperature of melting equals 307 K (peak) with the enthalpy of fusion 27.2 kJ·mol<sup>-1</sup>.

All remaining ILs reveal glass transition temperature ranging from 167.7 K ([BMPYR][FSI]) to 204.7 K ([OiQuin][FSI]).

**Effect of temperature on density, viscosity and surface tension.** The experimental data of density,  $\rho$  and dynamic viscosity,  $\eta$  as a function of temperature are listed in Table S1 in the SI. The parameters of correlation with  $R^2 = 1$  according to eqn. 2 ( $a_0$  and  $a_1$ ) are listed in Table S3 in the SI.

$$\rho = a_1 T + a_0 \quad (2)$$

The densities of all ILs decreases with an increase of temperature. The densities of ILs ranging in values from 1.1646 g·cm<sup>-3</sup> at  $T = 298.15$  K ([N<sub>2228</sub>][FSI]) to 1.3064 g·cm<sup>-3</sup> at  $T = 298.15$  K ([BMPYR][FSI]). At all temperatures density of the ILs increases in order: [N<sub>2228</sub>][FSI] < [OiQuin][FSI] < [HMMOR][FSI] < [BMPYR][FSI]. The data are shown in Fig. 2.

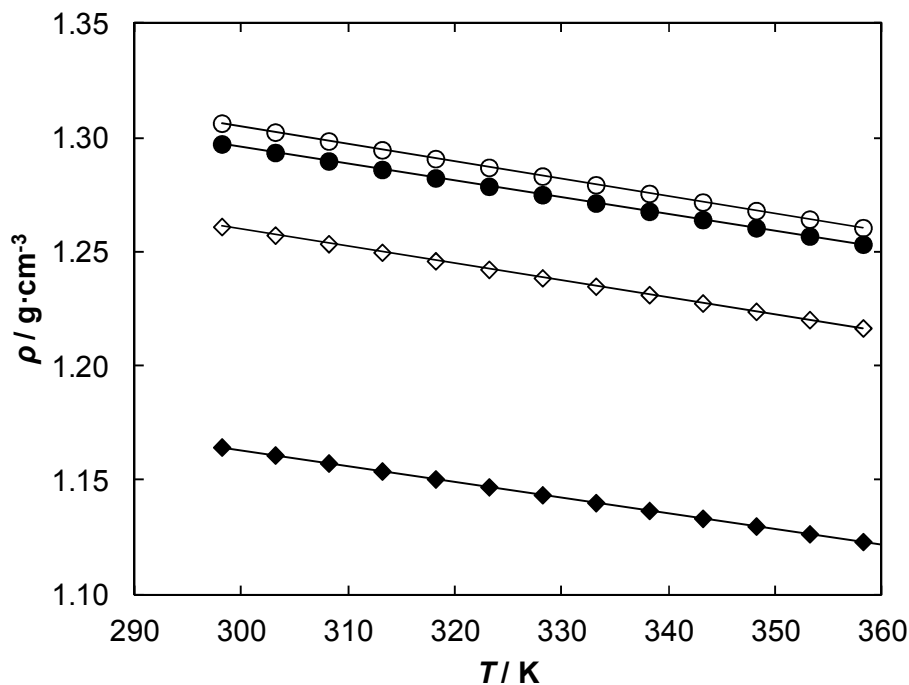


**Figure 2.** Density,  $\rho$ , for the tested ILs as a function of temperature: (●) [HMMOR][FSI]; (◇) [OiQuin][FSI]; (○) [BMPYR][FSI]; (◆) [N<sub>2228</sub>][FSI]. Solid lines represent eqns. given in Table S3 in the SI.

Dynamic viscosity of the pure ILs as a function of temperature was correlated by the well-known Vogel-Fulcher-Tammann, VFT equation:<sup>41-43</sup>

$$\eta = CT^{0.5} \exp\left(\frac{D}{T-T_0}\right) \quad (3)$$

The three correlation parameters of the eqn. (3) are listed in Table S4 in the SI. In this work, the parameter  $T_0$  was assumed to be ( $T_g - 60$  K). The dynamic viscosity as a function of temperature is shown in Fig. 3. The temperature dependence of viscosity becomes distinctly nonlinear, especially at high temperatures.

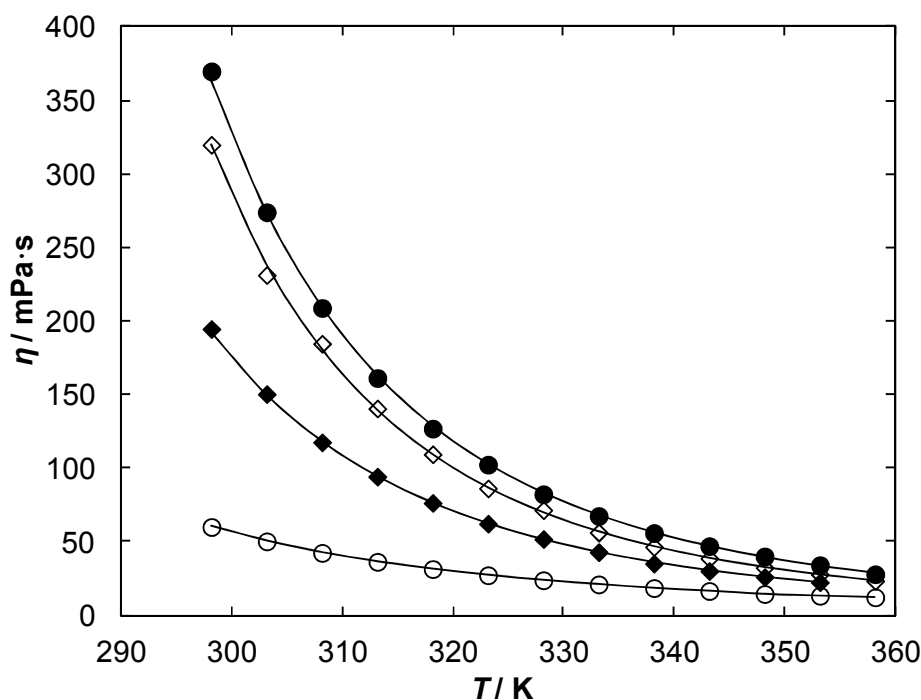


**Figure 3.** Dynamic viscosity,  $\eta$ , for the tested ILs as a function of temperature: (●) [HMMOR][FSI]; (◇) [OiQuin][FSI]; (○) [BMPYR][FSI]; (◆) [N<sub>2228</sub>][FSI]. Solid lines are calculated from VFT equation with parameters listed in Table S4 in the SI.

The values of surface tension,  $\sigma$ , are listed in Table S1 in the SI. Within the present study, the surface tension of all ILs are in the same range as other ILs, for example imidazolium ILs.<sup>44</sup> At all temperatures surface tension of the ILs increases in order: [OiQuin][FSI] = [N<sub>2228</sub>][FSI] < [HMMOR][FSI] < [BMPYR][FSI]. To compare the surface tension of [BMPYR][FSI] is 34.17 mN·m<sup>-1</sup> and measured earlier by us of [BMPYR][TCM] was 48.04 mN·m<sup>-1</sup> at  $T = 308.15$  K.<sup>45</sup> The surface tension increases with decreasing temperature, which is observed for all organic solvents. The data are shown in Fig. 4.

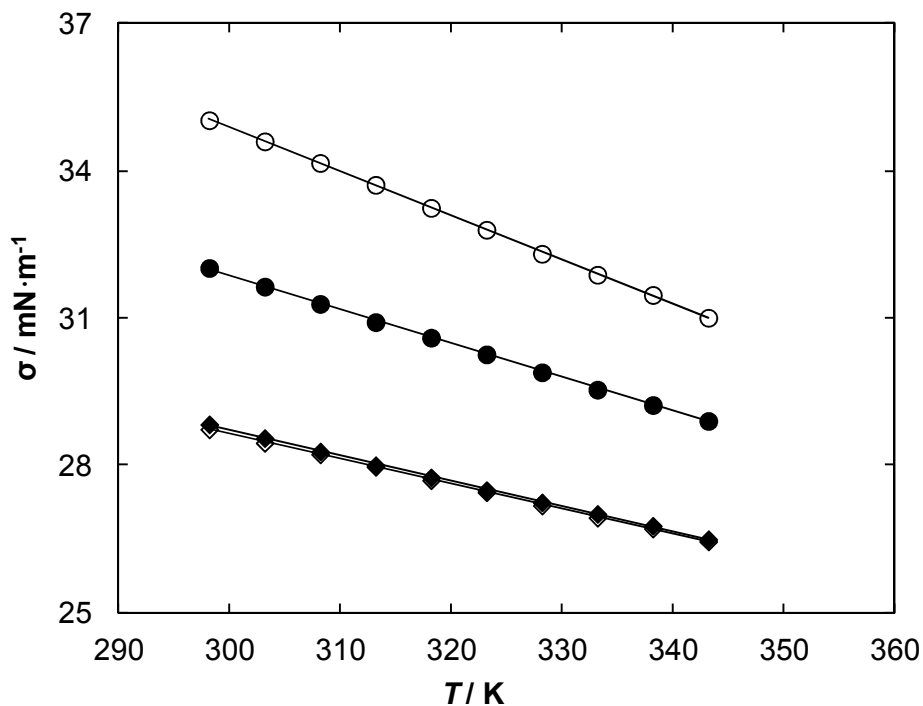


**Figure 4.** Surface tension,  $\sigma$ , for the tested ILs as a function of temperature: (●) [HMMOR][FSI]; (◇) [OiQuin][FSI]; (○) [BMPYR][FSI]; (◆) [N<sub>2228</sub>][FSI]. Solid lines represent eqns. given in Table S5 in the SI.

The results of regression analysis of the surface tension as a function of temperature was correlated by using eqn. 4 with parameters listed in Table S5 in the SI.

$$\sigma = b_1 T + b_0 \quad (4)$$

The surface thermodynamic functions may be calculated in the measured temperature range (298.15 to 343.15) K. The surface entropy, ( $S^\sigma$ ) and the surface enthalpy, ( $H^\sigma$ ) was calculated from the equations:<sup>46,47</sup>

$$S^\sigma = - \frac{d\sigma}{dT} \quad (5)$$

$$H^\sigma = \sigma - T \left( \frac{d\sigma}{dT} \right) \quad (6)$$

The thermodynamic functions for ILs at  $T = 298.15$  K are listed in Table 3. The surface entropies are as for many ILs in a range from  $S^\sigma = 19.34 \pm 0.05 \cdot 10^{-6} \text{ N}\cdot\text{m}^{-1}\cdot\text{K}^{-1}$  for [OiQuin][FSI] to  $30.51 \pm 0.05 \cdot 10^{-6} \text{ N}\cdot\text{m}^{-1}\cdot\text{K}^{-1}$  for [BMPYR][FSI] but are lower than that for [EMIM][TCM] for example ( $S^\sigma = 10.61 \pm 0.08 \cdot 10^{-5} \text{ N}\cdot\text{m}^{-1}\cdot\text{K}^{-1}$  at  $T = 298.15$  K)<sup>48</sup> and slightly lower than that for [BMPYR][TCM] ( $S^\sigma = 55.00 \pm 0.05 \cdot 10^{-6} \text{ N}\cdot\text{m}^{-1}\cdot\text{K}^{-1}$  at  $T = 308.15$  K).<sup>45</sup> The lower surface entropy is a picture of the lower organization of molecule at the surface. The surface enthalpies range from  $H^\sigma = 60.54 \pm 0.05 \cdot 10^{-2} \text{ N}\cdot\text{m}^{-1}$  for [OiQuin][FSI] to  $H^\sigma = 94.47 \pm 0.05 \cdot 10^{-2} \text{ N}\cdot\text{m}^{-1}$  for [BMPYR][FSI]. For comparison the value of [BMPYR][TCM]

was ( $H^\sigma = 64.98 \pm 0.05 \cdot 10^{-3} \text{ N}\cdot\text{m}^{-1}$  at  $T = 308.15 \text{ K}$ )<sup>45</sup> and is higher than those observed for [EMIM][TCM]<sup>48</sup> and for many other ILs.<sup>44</sup>

The critical temperature, ( $T_c$ ) of ILs may be calculated from the measurements of surface tension as a function of temperature according to two equations:

$$\sigma \left( \frac{M}{\rho} \right)^{2/3} = K (T_c^E - T) \quad (7)$$

$$\sigma = E^\sigma \left( 1 - \frac{T}{T_c^G} \right)^{11/9} \quad (8)$$

where  $K$  is a constant, and  $\rho$  ( $\text{g}\cdot\text{cm}^{-3}$ ) is density,  $M$  ( $\text{g}\cdot\text{mol}^{-1}$ ) is molecular mass,  $T$  (K) is the temperature of the measured surface tension  $\sigma$  ( $\text{N}\cdot\text{m}^{-1}$ ) and  $T_c^E$  (K) is the Eötvös critical temperature,<sup>49</sup>  $E^\sigma$  is the total surface energy and  $T_c^G$  is the Guggenheim critical temperature.<sup>50</sup>

The critical temperature of organic solvents is usually calculated from the van der Waals-Guggenheim equation (eqn. 8),<sup>50,51</sup> but it is also proposed for ILs. According to the corresponding states correlations, in both eqns. (7 and 8) the surface tension becomes null at the critical temperature.<sup>50</sup>

The total surface energy of the IL and the critical temperatures are listed in Table 3. The values of  $T_c^E$  and  $T_c^G$ , obtained from two different equations differ slightly from each other, mainly for [N<sub>2228</sub>][FSI] ( $T_c^E$  (K) = 1005.2 and  $T_c^G$  (K) = 976.7). In general the values of new [FSI]-based ILs are similar to the literature values of different ILs.<sup>44,45,48</sup> The total surface energies of the [FSI]-based ILs are similar to the other ILs.<sup>44,45,48</sup>

**Table 3. Surface Thermodynamic Functions for the Tested ILs at Temperature  $T = 298.15$  K: Surface Excess Energy,  $S^\sigma$ , Surface Enthalpy,  $H^\sigma$ , Critical Temperature,  $T_c$ , and Surface Energy,  $E^\sigma$**

	$10^6 \cdot S^\sigma / (\text{N} \cdot \text{m}^{-1} \cdot \text{K}^{-1})$	$10^2 \cdot H^\sigma / (\text{N} \cdot \text{m}^{-1})$	$T_c^E / (\text{K})$	$T_c^G / (\text{K})$	$E^\sigma / (\text{mN} \cdot \text{m}^{-1})$
[HMMOR][FSI]	25.00	77.74	849.1	856.9	54.0
[OiQuin][FSI]	19.34	60.54	1014.6	985.1	44.6
[BMPYR][FSI]	30.51	94.47	750.3	769.3	63.8
[N <sub>2228</sub> ][FSI]	19.80	61.92	1005.2	976.7	45.0

The parachors of the ILs were calculated according to the definition (eqn. 9) using the measured densities and they are shown in Table S6 in the SI.

$$P = \frac{M\sigma^{1/4}}{\rho} \quad (9)$$

The obtained values are higher for the [OiQuin][FSI] and [N<sub>2228</sub>][FSI] than those for [HMMOR][FSI] and [BMPYR][FSI] but they are in a range of all ILs.<sup>44,45,48</sup> For comparison the parachor for [BMPYR][TCM] was  $616.2 \pm 0.1 (\text{mN} \cdot \text{m}^{-1})^{1/4} \cdot \text{cm}^3 \cdot \text{mol}^{-1}$  at  $T = 308.15$  K.<sup>48</sup>

**LLE in Binary systems.** PEA is soluble in all [FSI]-based ILs in the whole mole fraction region from zero to one at  $T = 308.15$  K. The results of the solubility of [FSI]-based ILs in water are shown in Table S7 in the SI. The temperatures,  $T^{\text{LLE}}$  versus the IL mole fraction,  $x_1$  obtained with two methods: dynamic (synthetic) in the IL-rich phase and conductivity method in the water-rich phase is presented in Table S7 in the SI. Based on Fig. 5 we can see the large miscibility gap for all ILs with UCST, which was expected for

hydrophobic ILs. The largest immiscibility envelope was observed for [N<sub>2228</sub>][FSI] and the smallest for [HMMOR][FSI].

The solubility of the IL in water (at the water rich phase) increases in order: [N<sub>2228</sub>][FSI] < [HMMOR][FSI] < [BMPYR][FSI] < [OiQuin][FSI]. The [OiQuin][FSI] has the largest interaction with water and reveals the largest solubility in water. The solubility of water in the IL (at the IL rich phase) increases in different order: [N<sub>2228</sub>][FSI] < [OiQuin][FSI] < [BMPYR][FSI] < [HMMOR][FSI]. The solubility of water in IL [HMMOR][FSI] at  $T = 308.15$  K was  $x_1 = 0.645$  ( $x_2 = 0.355$ ) and that of IL in water was  $x_1 = 0.22 \times 10^{-3}$ . The miscibility gap in all systems underlines the small interaction of the IL and water, which is expected for ILs used for the extraction from aqueous phase. For all ILs the Upper Critical Solution Temperature (UCST) is observed. Unfortunately, the maximum is at much higher temperatures than our experiment. The largest loop of immiscibility is observed for the ammonium-based IL, [N<sub>2228</sub>][FSI].

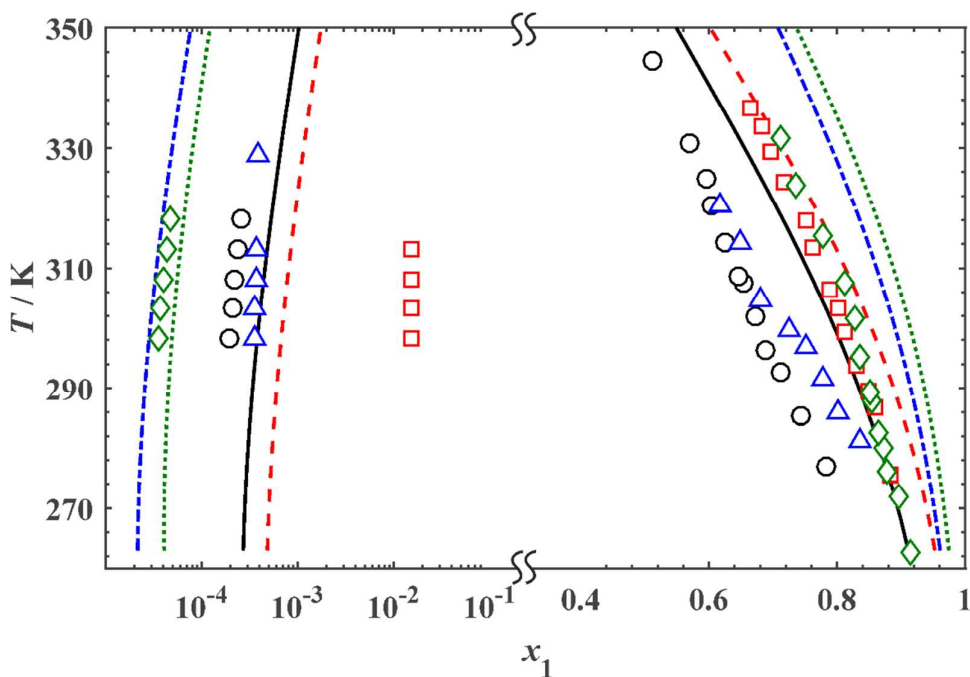


**Figure 5.** Experimental data vs COSMO-RS predictions of LLE in binary systems {IL (1) + water (2)} at pressure  $p = 101$  kPa. Markers designated by experimental data: (○),

[HMMOR][FSI]; ( $\square$ ), [OiQuin][FSI]; ( $\Delta$ ), [BMPYR][FSI]; ( $\diamond$ ), [N<sub>2228</sub>][FSI]. Lines designated by COSMO-RS calculations: (—), [HMMOR][FSI]; (- - -), [OiQuin][FSI]; (— - —), [BMPYR][FSI]; (...), [N<sub>2228</sub>][FSI].

Experimental data in comparison with COSMO-RS predictions of LLE in binary systems {IL (1) + water (2)} at pressure  $p = 101$  kPa shows that the character of temperature dependencies is well described and the qualitative description is quite well.

**LLE in ternary systems.** The measured tie-lines in ternary mixtures {IL (1) + PEA (2) + H<sub>2</sub>O (3)} at  $T = 308.15$  K and  $p = 101$  kPa are given in Table 4. The ternary LLE data are presented in a form of the Gibbs triangles in Fig. 6 as an example and in Figs. S5-S7 in the SI. They show clearly the immiscibility region in ternary systems. These figures show that the miscibility gap is the largest for [N<sub>2228</sub>][FSI] because of the lowest solubility of water in the IL. It may be the result of octane chain at the cation of the IL. There are no differences to our earlier measurements in solubility of water in PEA. The one phase region is from  $x_2 = 0.582$  as it was observed by us earlier.<sup>18-22</sup> In binary systems {IL (1) + PEA (2)} the complete miscibility is present in the Gibbs triangles in all mixtures.

The process of extraction is controlled by two parameters, calculated from tie-lines, the distribution ratio of PEA ( $\beta_2$ ) and the selectivity of PEA extraction ( $S_{23}$ ). These parameters are defined by the following expressions:

$$\beta_2 = \frac{x_2^{\text{II}}}{x_2^{\text{I}}} \quad (10)$$

$$S_{23} = \frac{x_2^{\text{II}} \cdot x_3^{\text{I}}}{x_2^{\text{I}} \cdot x_3^{\text{II}}} \quad (11)$$

where  $x$  is the mole fraction; superscripts I and II refer to water-rich phase and ionic liquid-rich phase, respectively. Subscripts 2 and 3 refer to PEA and

water, respectively. The values of  $\beta_2$  and  $S_{23}$  are listed in Table 4, together with the experimental equilibrium data in ternary systems.

**Table 4. Experimental LLE Data Summary for Ternary System {IL (1) + 2-Phenylethanol (PEA) (2) + water (3)} at  $T = 308.15$  K and pressure  $p = 101$  kPa: Tie-lines Mole Fractions of Water- and IL-rich Phases ( $x_i^W$  and  $x_i^{IL}$ , respectively), Solute Distribution Ratios of PEA ( $\beta_2$ ) and PEA/Water Selectivities ( $S_{23}$ )**

water-rich phase		IL-rich phase		$\beta_2$	$S_{23}$
$x_1^W$	$x_2^W$	$x_1^{IL}$	$x_2^{IL}$		
[HMMOR][FSI]					
0.000	0.000	0.721	0.000		
0.000	0.001	0.686	0.048	48.00	180.3
0.000	0.001	0.586	0.115	115.0	384.2
0.000	0.002	0.492	0.236	118.0	433.0
0.000	0.002	0.426	0.273	136.5	452.6
0.000	0.002	0.359	0.298	149.0	433.5
0.000	0.002	0.138	0.479	239.5	624.1
0.000	0.003	0.082	0.528	176.0	449.9
0.000	0.003	0.036	0.573	191.0	487.0
0.000	0.004	0.000	0.582	145.5	346.7
[OiQuin][FSI]					
0.000	0.001	0.694	0.000		
0.000	0.001	0.665	0.030	30.00	98.3
0.000	0.001	0.537	0.138	138.0	424.2
0.000	0.002	0.449	0.216	108.0	321.7
0.000	0.003	0.315	0.354	118.0	355.4
0.000	0.003	0.250	0.403	134.3	386.0
0.000	0.003	0.156	0.456	152.0	390.6
0.000	0.003	0.151	0.460	153.3	393.0
0.000	0.003	0.086	0.516	172.0	430.9
0.000	0.004	0.000	0.582	145.5	346.7
[BMPYR][FSI]					
0.000	0.000	0.679	0.000		
0.000	0.001	0.646	0.008	8.00	23.1
0.000	0.001	0.609	0.019	19.0	51.0
0.000	0.001	0.529	0.100	100.0	269.3
0.000	0.001	0.457	0.184	184.0	512.0
0.000	0.002	0.383	0.232	116.0	300.7
0.000	0.002	0.316	0.279	139.5	343.8
0.000	0.003	0.291	0.312	104.0	260.5
0.000	0.003	0.122	0.451	150.3	351.0
0.000	0.003	0.099	0.470	156.7	362.4
0.000	0.003	0.058	0.498	166.0	372.8
0.000	0.004	0.042	0.508	127.0	281.7
0.000	0.004	0.000	0.582	145.5	346.7

[N <sub>2228</sub> ][FSI]					
0.000	0.000	0.708	0.000		
0.000	0.002	0.605	0.065	32.5	98.3
0.000	0.002	0.478	0.197	98.5	302.5
0.000	0.004	0.466	0.203	50.8	152.7
0.000	0.004	0.310	0.349	87.3	254.8
0.000	0.004	0.320	0.338	84.5	246.1
0.000	0.005	0.234	0.419	83.8	240.3
0.000	0.005	0.196	0.439	87.8	239.3
0.000	0.007	0.127	0.489	69.9	180.6
0.000	0.007	0.115	0.495	70.7	180.0
0.000	0.004	0.000	0.582	145.5	346.7

\* Standard uncertainties are:  $u(x) = \pm 0.003$ ;  $u(T) = \pm 0.1$  K;  $u(p) = \pm 0.1$  kPa.

The parameters of  $\beta_2$  and  $S_{23}$  are different for different tie-lines. They depend strongly on the alkane chain length in the cation of the IL. The average solute distribution ratio increases in the following order: [BMPYR][FSI] ( $\beta_{av} = 118$ ) < [OiQuin][FSI] ( $\beta_{av} = 128$ ) < [HMMOR][FSI] ( $\beta_{av} = 147$ ) < [N<sub>2228</sub>][FSI] ( $\beta_{av} = 224$ ). Usually, the longer aliphatic chain, the larger solute distribution ratio and lower selectivity. In this work, butyl- substituent at the cation revealed lower  $\beta_{av}$  than those for hexyl-, or octyl- chain. The comparison with the ILs of the same cation and [NTf<sub>2</sub>]<sup>-</sup> anion is not showing huge differences for [BMPYR][NTf<sub>2</sub>] ( $\beta_{av} = 133$ ),<sup>23</sup> or for [HMMOR][NTf<sub>2</sub>] ( $\beta_{av} = 149$ ),<sup>21</sup> or for [N<sub>2228</sub>][NTf<sub>2</sub>] ( $\beta_{av} = 209$ ).<sup>20</sup> The larger difference is observed in comparison with [OiQuin][NTf<sub>2</sub>] ( $\beta_{av} = 200$ ).<sup>18</sup> The largest  $\beta_{av}$  were observed for tetracyanoborate-based ILs, for example for [BMPYR][TCB] ( $\beta_{av} = 241$ ).<sup>22</sup>

The average selectivity of extraction of PEA from water is the highest for [HMMOR][FSI]. It increases in the following order: [N<sub>2228</sub>][FSI] ( $S_{av} = 81$ ) < [BMPYR][FSI] ( $S_{av} = 290$ ) < [OiQuin][FSI] ( $S_{av} = 350$ ) < [HMMOR][FSI] ( $S_{av} = 421$ ). These results are much lower than those obtained for ILs with [NTf<sub>2</sub>]<sup>-</sup> anion. Previously obtained data are: for [BMPYR][NTf<sub>2</sub>] ( $S_{av} = 367$ ),<sup>23</sup> for [HMMOR][NTf<sub>2</sub>] ( $S_{av} = 389$ )<sup>21</sup> for

[N<sub>2228</sub>][NTf<sub>2</sub>] ( $S_{av} = 711$ ),<sup>20</sup> and for [Quin][NTf<sub>2</sub>] ( $S_{av} = 795$ ).<sup>18</sup> The selectivities of measured by us earlier tetracyanoborate-based ILs were much lower.<sup>22</sup>

The analysis of our literature data shows that the best suitable ILs for the separation of PEA from aqueous phase are [N<sub>2228</sub>][NTf<sub>2</sub>] or [OiQuin][NTf<sub>2</sub>]. New anion proposed by us in this work presents average  $\beta_{av}$  and  $S_{av}$  in comparison with all data reported by us earlier. New values are also lower than those, obtained for ILs with [NTf<sub>2</sub>]<sup>-</sup> anion.

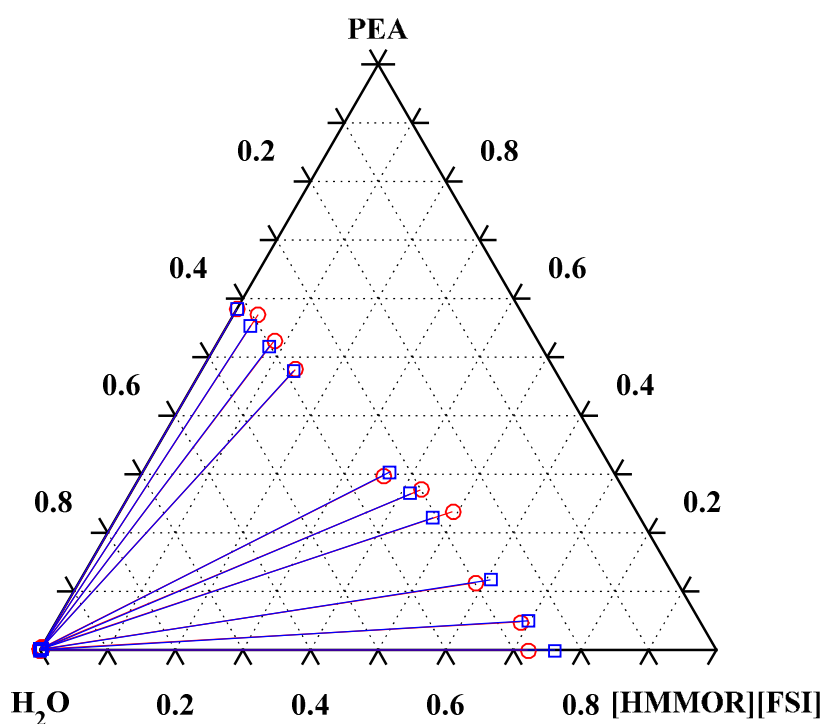


**Figure 6.** Experimental *versus* COSMO-RS predictions of LLE tie-lines for ternary system {[HMMOR][FSI] (1) + PEA (2) + water (3)} at  $T = 308.15$  K and pressure  $p = 101$  kPa; ( $\circ$ — $\circ$ ) experimental data, ( $\square$ — $\square$ ) COSMO-RS predictions.

**Data correlation.** The correlation method based on the NRTL model, describing the excess Gibbs energy is proposed for LLE binary and ternary data correlation.<sup>52,53</sup>

$$\frac{G^E}{RT} = x_1 x_2 \left[ \frac{\tau_{21} G_{21}}{x_1 + x_2 G_{21}} + \frac{\tau_{12} G_{12}}{G_{12} x_1 + x_2} \right] \quad (12)$$

The model adjustable parameters  $\tau_{21}$  and  $\tau_{12}$  were found by method described in our previous work.<sup>19</sup> For ternary systems there are three parameters of the NRTL model per a pair of components  $i$  and  $j$ . The nonrandomness parameter  $\alpha_{ij} = \alpha_{ji}$  was set as constants (0.2, or 0.35), whereas the binary interaction parameters were temperature dependent according to formulas:

$$\tau_{ij} = a_{ij} + b_{ij} \left( \frac{1}{T} - \frac{1}{T_0} \right) + c_{ij} (T - T_0) \quad (13)$$

$$\tau_{ji} = a_{ji} + b_{ji} \left( \frac{1}{T} - \frac{1}{T_0} \right) + c_{ji} (T - T_0) \quad (14)$$

where  $T_0 = 308.15$  K is a reference temperature used in the LLE ternary measurements. The equation parameters and corresponding root-mean-square deviations (eqn. 15) are listed in Table 5.

$$RMSD = \left( \sum_i \sum_l \sum_m [w_{ilm}^{\text{exp}} - w_{ilm}^{\text{calc}}]^2 / 6k \right)^{1/2} \quad (15)$$

where  $w$  is the mass fraction and the subscripts  $i$ ,  $l$ , and  $m$  designate the component, phase, and tie-line, respectively. The experimental and calculated LLE data agreed relatively well (see Figs. 6 and Figs. S5-S7 in the SI). The model accurately represents the measured data. The RMSD of equilibrium mole fraction is at the level of 0.001. This good result was obtained by the applying temperature-dependence of the parameters.

**Table 5. NRTL Model Parameters  $\tau_{ij}$  and  $\tau_{ji}$  Used in LLE Calculations for Systems {IL (1) + PEA (2) + Water (3)} and the Root Mean Square Deviations (RMSDs) between Calculated and Experimental Equilibrium Mole Fractions**

$i-j$	$\tau_{ij}^a$		$\tau_{ij}^b$				$\alpha_{ij} = \alpha_{ji}$	RMSD
	$a_{ij}$	$10^{-3}b_{ij} / \text{K}$	$c_{ij} / \text{K}^{-1}$	$a_{ji}$	$10^{-3}b_{ji} / \text{K}$	$c_{ji} / \text{K}^{-1}$		
[HMMOR][FSI] (1) + PEA (2) + water (3)								
1-2	0.491			6.286			0.20	0.0191
1-3	-0.519	1.899		8.581	-0.356		0.20	0.0052
2-3	0.774	-3.215	-0.0401	4.920	-3.162	-0.0323	0.35	0.0013
[BMPYR][FSI] (1) + PEA (2) + water (3)								
1-2	2.672			-5.495			0.20	0.0117
1-3	0.070	-8.488	-0.1160	8.998	2.035	0.0328	0.20	0.0081
2-3	0.774	-3.215	-0.0401	4.920	-3.162	-0.0323	0.35	0.0013
[OiQuin][FSI] (1) + PEA (2) + water (3)								
1-2	-3.363			-4.125			0.20	0.0068
1-3	0.126	0.848	-0.0105	4.137	0.513	0.0216	0.20	0.0031
2-3	0.774	-3.215	-0.0401	4.920	-3.162	-0.0323	0.35	0.0013
[N <sub>822</sub> ][FSI] (1) + PEA (2) + water (3)								
1-2	11.515			-8.474			0.20	0.0176
1-3	0.470	-0.713	-0.0276	9.501	1.775	0.0181	0.20	0.0063
2-3	0.774	-3.215	-0.0401	4.920	-3.162	-0.0323	0.35	0.0013

**Data prediction.** Experimental data in comparison with COSMO-RS predictions of LLE in binary systems {IL (1) + water (2)} at pressure  $p = 101$  kPa showed in Fig. 5 present quite good similarity. The area of miscibility gap follows the trend of experimental points. The corresponding values of RMSD (eqn.15) between the calculated and experimental mole

1  
2  
3 fractions are 0.0915, 0.0331, 0.1443, 0.0788 for [HMMOR][FSI], [OiQuin][FSI],  
4  
5 [BMPYR][FSI] and [N<sub>2228</sub>][FSI], respectively.  
6

7  
8 As seen from Figs. 6 and S5-S7 in the SI, the COSMO-RS method with the  $\sigma$ -profiles  
9  
10 presented in Fig. 1 provide satisfactory predictions of LLE in the systems under study. The  
11  
12 corresponding values of RMSD (eqn.15) between the calculated and experimental mole  
13  
14 fractions were 0.0047, 0.0243, 0.0231 and 0.0252 for the ternary systems with  
15  
16 [HMMOR][FSI], [OiQuin][FSI], [BMPYR][FSI] and [N<sub>2228</sub>][FSI], respectively. IL-rich phase  
17  
18 compositions are, however, overpredicted. Furthermore, the model does not capture an impact  
19  
20 of cation on LLE in binary systems {IL + water}; according to our COSMO-RS calculations,  
21  
22 miscibility gap with water increases as follows: [HMMOR][FSI] < [BMPYR][FSI] <  
23  
24 [OiQuin][FSI] < [N<sub>2228</sub>][FSI]. This suggest that the COSMO-RS outcomes should be treated  
25  
26 with care, when applied in computer-aided molecular design of novel ILs for separating  
27  
28 value-added chemicals like PEA from their aqueous solutions.  
29  
30  
31  
32  
33

### 34 ■ Conclusions

35  
36  
37 The synthesis, thermal (DSC) and physico-chemical properties (density, dynamic viscosity  
38  
39 and surface tension) of four new ionic liquids is presented. The liquid-liquid phase  
40  
41 equilibrium in binary systems for mixtures of ILs ([HMMOR][FSI], [OiQuin][FSI],  
42  
43 [BMPYR][FSI] and [N<sub>2228</sub>][FSI]) with PEA, or water have been measured. On the basis of  
44  
45 these investigations, we may conclude that new ILs proposed by us may be interesting for the  
46  
47 extraction of PEA from water-phase. These ILs exhibit complete miscibility with PEA and  
48  
49 immiscibility with water. Four new ternary systems of {IL + PEA + water} were presented at  
50  
51 temperature  $T = 308.15$  K and  $p = 101$  kPa. Systems under study exhibited Treybal's Type II  
52  
53 behaviour with complete miscibility in binary system (IL + PEA). The ILs capacity, described  
54  
55 in terms of the solute distribution ratio and of selectivity coefficients were calculated and  
56  
57  
58  
59  
60

1  
2  
3 compared to the published data for PEA extraction from water. Relatively, the highest values  
4  
5 of capacity and selectivity may suggest that the [HMMOR][FSI] may be used as an entrainer.  
6  
7 However, the separation parameters of [HMMOR][FSI] are lower than those for [N<sub>2228</sub>][NTf<sub>2</sub>]  
8  
9 and [C<sub>8</sub>iQuin][NTf<sub>2</sub>] ILs.  
10

11  
12 The NRTL and the COSMO-RS models were demonstrates as interesting thermodynamic  
13  
14 tools for correlation and prediction the binary IL/water and ternary IL/PEA/water systems. In  
15  
16 particular, the NRTL model presented low RMSD in ternary LLE. It was shown that  
17  
18 parameters obtained in binary data can be transferred to correlate the ternary tie-lines. The  
19  
20 obtained results of prediction confirms also the ability of COSMO-RS to model the extraction  
21  
22 behaviour of new systems with ILs. In conclusion we hope that our new experimental data  
23  
24 and modelling results will be useful for designing ILs as new entrainers for modern extraction  
25  
26 technologies.  
27  
28  
29  
30

### 31 **Appendix A. Supporting Information**

32  
33 Supporting Information related to this article can be found, in the online version, at  
34  
35 <http://dx.doi.org/>, Reports S1-S5, details for synthesis, NMR, elemental analysis and purity;  
36  
37 Figures S1-S4, DSC thermograms of ILs; Table S1 density, dynamic viscosity and surface  
38  
39 tension; Table S2 operational conditions for GC analysis; Tables S3, S4 and S5 summarizing  
40  
41 some additional parameters of correlation of density, viscosity and surface tension; Table S6  
42  
43 presents Parachor as a function of temperature; Table S7 presents LLE in binary systems {IL  
44  
45 (1) + Water (2)}; Figures S5-S7 show ternary LLE diagrams with COSMO-RS calculations.  
46  
47  
48  
49  
50

### 51 **■AUTHOR INFORMATION**

#### 52 **Corresponding Author**

53  
54  
55 \* E-mail: ula@ch.pw.edu.pl. Phone: (+48) 22-6213115. Fax: (+48) 22-6282741.  
56  
57

#### 58 **Notes**

1  
2  
3 The authors declare no competing financial interest.  
4

#### 5 ■ ACKNOWLEDGEMENTS

6  
7 This work has been supported by the project of National Science Center in Poland for years  
8  
9 2015-2018, No. 201/15/B/ST5/00136.  
10  
11

#### 12 ■ REFERENCES

13  
14  
15  
16 (1) Etschmann, M.M.W.; Sell, D.; Schrade, J. Screening of yeasts for the production of the  
17  
18 aroma compound 2-phenylethanol in a molasses-based medium. *Biotechn. Lett.* **2003**, *25*,  
19  
20 531–536.  
21

22  
23 (2) Stark, D.; Münch, T.; Sonnleitner, B.; Marison, I.W.; von Stockar, U. Novel type of in  
24  
25 situ extraction: Use of solvent containing microcapsules for the bioconversion of 2-  
26  
27 phenylethanol from L-phenylalanine by *Saccharomyces cerevisiae*. *Biotechn. Bioeng.* **2003**,  
28  
29 *83*, 376-385.  
30

31  
32 (3) Wang, H.; Dong, Q.; Meng, Ch.; Shi, X.; Guo, Y. A continuous and adsorptive bioprocess  
33  
34 for efficient production of the natural aroma chemical 2-phenylethanol with yeast. *Enzyme*  
35  
36 *Microb. Technol.* **2011**, *48*, 404-407.  
37

38  
39 (4) Mei, J.; Min, H.; Lü, Z. Enhanced biotransformation of L-phenylalanine to 2-  
40  
41 phenylethanol using an in situ product adsorption technique. *Proc. Biochem.* **2009**, *44*, 886-  
42  
43 890.  
44

45  
46 (5) Hua, D.L.; Lin, S.; Li, Y.F.; Zhang, Z.B.; Chen, Y.; Chen, H. et al. Enhanced 2-  
47  
48 phenylethanol production from L-phenylalanine via in situ product adsorption. *Biocatal.*  
49  
50 *Biotransfor.* **2010**, *28*, 259-266.  
51

52  
53 (6) Rong, S.; Ding, B.; Zhang, X.; Zheng, X.; Wang, Y. Enhanced biotransformation of 2-  
54  
55 phenylethanol with ethanol oxidation in a solid-liquid two phases system by active dry yeast.  
56  
57 *Curr. Microbiol.* **2011**, *6*, 503-509.  
58  
59  
60

- 1  
2  
3 (7) Gao, F.; Daugulis, A.J. Bioproduction of the aroma compound 2-phenylethanol in a solid-  
4 liquid two-phase partitioning bioreactor system by *Kluyveromyces marxianus*. *Biotechn.*  
5 *Bioeng.* **2009**, *104*, 332-339.  
6  
7  
8  
9  
10 (8) Michal, M.; Goncalves, R.F.; Markoš, J. Intensive 2-phenylethanol production in a hybrid  
11 system combined of a stirred tank reactor and an immersed extraction membrane module.  
12 *Chemical Papers* **2014**, *68*, 1656-1666.  
13  
14  
15  
16 (9) Domańska, U. General reviews of ionic liquids and their properties. In M. Koel, Ed. *Ionic*  
17 *Liquids in Chemical Analysis*; CRC Press, Taylor and Francis Group: Abingdon, UK, 2008.  
18  
19  
20 (10) Fan, L-L.; Li, H-J.; Chen, Q-H. Applications and mechanisms of ionic liquids in whole-  
21 cell biotransformation. *Int. J. Mol. Sci.* **2014**, *15*, 12196-12216.  
22  
23  
24  
25 (11) Canales, R.I.; Brennecke, J.F. Comparison of ionic liquids to conventional organic  
26 solvents for extraction of aromatics from aliphatics. *J. Chem. Eng. Data* **2016**, *61*, 1685-1699.  
27  
28  
29  
30 (12) Hansmeir AR, Meindersma GW, de Haan AB. Desulfurization and denitrogenation of  
31 gasoline and diesel fuels by means of ionic liquids. *Green Chem.* **2011**, *3*, 1907-13.  
32  
33  
34  
35 (13) Domańska, U.; Wlazło, M. Effect of the cation and anion of the ionic liquid on  
36 desulfurization of model fuels. *Fuel* **2014**, *134*, 114-125.  
37  
38  
39  
40 (14) Nann, A.; Held, Ch.; Sadowski, G. Liquid-liquid equilibria of 1-butanol/water/IL  
41 systems. *Ind. Eng. Chem. Res.* **2013**, *52*, 18472-18481.  
42  
43  
44 (15) Neves, C.M.S.S.; Granjo, J.F.O.; Freire, M.F.; Robertson, A.; Oliviera, N.M.C.; J.A.P.  
45 Coutinho, J.A.P. Separation of ethanol-water mixtures by liquid-liquid extraction using  
46 phosphonium-based ionic liquids. *Green Chem.* **2011**, *13*, 1517-1526.  
47  
48  
49  
50 (16) Sendovski, M.; Nir, N.; Fishman, A. Bioproduction of 2-phenylethanol in a biphasic  
51 ionic liquid aqueous system. *J. Agric. Food Chem.* **2010**, *58*, 2260-2265.  
52  
53  
54  
55  
56  
57  
58  
59  
60

1  
2  
3 (17) Xiang, Z.Y.; LU, Y.C.; Zou, Y.; Gong, X.C. Luo, G.S. Preparation of microcapsules  
4 containing ionic liquids with a new solvent extraction system. *React. Funct. Polym.* **2008**, *68*,  
5 1260-1265.  
6  
7

8  
9 (18) Domańska, U.; Zawadzki, M.; Królikowski, M.; Lewandrowska, A. Phase equilibria  
10 study of binary and ternary mixtures of {*N*-octylisoquinolinium  
11 bis{(trifluoromethyl)sulfonyl}imide + hydrocarbon, or alcohol, or water. *Chem. Eng. J.* **2012**,  
12 *181-182*, 63-71.  
13  
14  
15  
16  
17

18  
19 (19) Domańska, U.; Patuszyński, K.; Królikowski, M.; Wróblewska, A. Separation of 2-  
20 phenylethanol from water by liquid-liquid extraction with ionic liquids: New experimental  
21 data and modeling with modern thermodynamic tools. *Ind. Eng. Chem. Res.* **2016**, *55*, 5736-  
22 5747.  
23  
24  
25  
26  
27

28 (20) Domańska, U.; Okuniewska, P.; Królikowski, M. Separation of 2-phenylethanol (PEA)  
29 from water using ionic liquids. *Fluid Phase Equilib.* **2016**, *423*, 109-119.  
30  
31  
32

33 (21) Domańska, U.; Królikowski, M.; Zawadzki, M.; Wróblewska, A. Phase equilibrium with  
34 ionic liquids and selectivity in separation of 2-phenylethanol from water. *J. Chem Thermodyn.*  
35 **2016**, *102*, 357-366.  
36  
37  
38  
39

40 (22) Królikowski, M.; Pachla, J.; Ramjugernath D.; Naidoo, P.; Domańska, U. Extraction of  
41 2-phenylethanol (PEA) from aqueous phase using tetracyanoborate-based ionic liquids. *J.*  
42 *Mol. Liq.* **2017**, *224*, 1124-1130.  
43  
44  
45  
46  
47

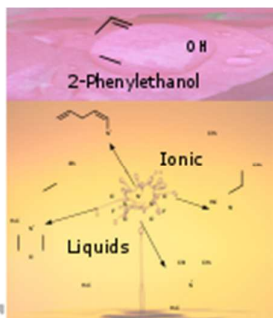
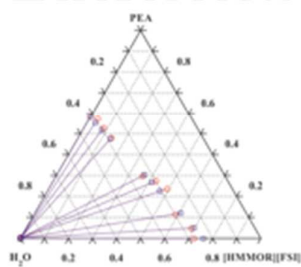
48 (23) Domańska, U.; Więckowski, M.; Okuniewska, P. Designing eutectic mixtures for the  
49 extraction of 2-phenylethanol (PEA) from aqueous phase. *Fluid Phase Equilib.* **2017**, *447*,  
50 84-94.  
51  
52  
53  
54

55 (24) Shkrob, I.A.; Marin, T.W.; Zhu, Y.; Abraham, D.P. Why Bis(fluorosulfonyl)imide is a  
56 “Magic Anion” for electrochemistry. *J. Phys. Chem. C* **2014**, *118*, 19661–19671.  
57  
58  
59  
60

- 1  
2  
3 (25) Fujii, K.; Seki, S.; Fukuda, S.; Takamuku, T.; Koharad, S.; Kameda, Y.; Umebayashi,  
4 Y.; Ishiguro, Y. Liquid structure and conformation of a low-viscosity ionic liquid, *N*-methyl-  
5 *N*-propyl-pyrrolidinium bis(fluorosulfonyl) imide studied by high-energy X-ray scattering. *J.*  
6 *Mol. Liquids* **2008**, 143, 64-69.
- 7  
8  
9  
10  
11  
12 (26) Fujii, K.; Seki, S.; Fukuda, S.; Kanzaki, R.; Takamuku, T.; Umebayashi, Y.; Ishiguro, S.  
13 Anion conformation of low-viscosity room-temperature ionic liquid 1-ethyl-3-  
14 methylimidazolium bis(fluorosulfonyl) imide. *J. Phys. Chem. B* **2007**, 111, 12829–12833.
- 15  
16  
17  
18  
19  
20 (27) Yoon, Y.; Zhu, H.; Hervault, A.; Armand, M.; MacFarlane, D.R.; Forsyth, M.  
21 Physicochemical properties of *N*-propyl-*N*-methylpyrrolidinium bis(fluorosulfonyl)imide for  
22 sodium metal battery applications. *Phys. Chem. Chem. Phys.* **2014**, 16, 12350-12355.
- 23  
24  
25  
26 (28) Huh, C., Mason, S.G.: A rigorous theory of ring tensiometry. *Colloid Polym. Sci.* **1975**,  
27 253, 566-580.
- 28  
29  
30  
31 (29) Harkins, W.D.; Jordan, H.F. A method for determination of surface and interfacial  
32 tension from the maximum pull on a ring. *J. Am. Chem. Soc.* **1930**, 52, 1751-1772.
- 33  
34  
35 (30) Freud, B.B.; Freud, H.Z. A theory of the ring method for the determination of surface  
36 tension. *J. Am. Chem. Soc.* **1930**, 52, 1772-1782.
- 37  
38  
39  
40 (31) Kurnia, K.A.; Quental, M.V.; Santos, L.M.N.F., Freire, M.G.; Coutinho, J.A.P. Mutual  
41 solubilities between water and non-aromatic sulfonium-, ammonium- and phosphonium-  
42 hydrophobic ionic liquids. *Phys. Chem. Chem. Phys.* **2015**, 17, 4569 – 4577.
- 43  
44  
45  
46 (32) Klamt, A. Conductor-like screening model for real solvents: a new approach to the  
47 quantitative calculation of solvation phenomena. *J. Phys. Chem.* **1995**, 99, 2224–2235.
- 48  
49  
50  
51 (33) Klamt, A.; Eckert, F. COSMO-RS: a novel and efficient method for the a priori  
52 prediction of thermophysical data of liquids. *Fluid Phase Equilib.* **2000**, 172, 43–72.
- 53  
54  
55  
56  
57  
58  
59  
60

- 1  
2  
3 (34) Klamt, A. COSMO-RS: from quantum chemistry to fluid phase thermodynamics and  
4 drug design. Elsevier, 2005.  
5  
6  
7 (35) Klamt, A.; Schüürmann, G. COSMO: a new approach to dielectric screening in solvents  
8 with explicit expressions for the screening energy and its gradient. *J. Chem. Soc. Perkin*  
9 *Trans.* **1993**, 2, 799–805.  
10  
11  
12 (36) Eckert, F.; Klamt, A. COSMOtherm (v. C3.0, release 17.01), COSMOlogic GmbH& Co.  
13 KG, Leverkusen, Germany, 2017.  
14  
15  
16  
17 (37) Ahlrichs, R.; Bär, M.; Häser, M.; Horn, H.; Kölmel, C. Electronic structure calculations  
18 on workstation computers: The program system Turbomole. *Chem. Phys. Lett.* **1989**, 162,  
19 165–169.  
20  
21  
22  
23 (38) Pedrew, J.P. Density-functional approximation for the correlation energy of the  
24 inhomogeneous electron gas. *Phys. Rev. B* **1986**, 33, 8822–8824.  
25  
26  
27  
28 (39) Becke, A.D. Density-functional exchange-energy approximation with correct asymptotic  
29 behavior. *Phys. Rev. A* **1988**, 38, 3098–3100.  
30  
31  
32  
33 (40) Schafer, A.; Huber C.; Alrichs, R. Fully optimized contracted Gaussian basis sets of  
34 triple-zeta valence quality for atoms Li to Kr. *J. Chem. Phys.* **1994**, 100, 5829–5835.  
35  
36  
37  
38 (41) Vogel, H.: Das temperaturabhängigkeitgesetz der viskositat von flussifkeiten (the  
39 temperature dependence of the viscosity of liquids). *Phys. Z.* **1921**, 22, 645-646.  
40  
41  
42  
43 (42) Fulcher, G.C. Analysis of recent measurements of the viscosity of glasses. *J. Am.*  
44 *Ceram. Soc.* **1925**, 8, 339-355.  
45  
46  
47  
48 (43) Tammann, G., Hesse, H. Die abhangingkeit der viskositat von der temperatur bei  
49 unterkühlten flussigkeiten (The dependence of the viscosity on temperature for super-cooled  
50 liquids). *Z. Anorg. Allg. Chem.* **1926**, 156, 245-257.  
51  
52  
53  
54  
55  
56  
57  
58  
59  
60

- 1  
2  
3 (44) Freire, M.G.F.; Carvalho, P.J.; Fernandes, A.M.; Marrucho, I.M.; Queimada, A.J.;  
4  
5 Coutinho, J.A.P. Surface tensions of imidazolium based ionic liquids: Anion, cation,  
6  
7 temperature and water effect. *J. Coll. Interf. Sci.* **2007**, *314*, 621-630.  
8  
9  
10 (45) Domańska, U., Królikowska, M., Walczak, K. Density, viscosity and surface tension of  
11  
12 binary mixtures of 1-butyl-1-methylpyrrolidinium tricyanomethanide with benzothiophene.  
13  
14 *J. Solution Chem.* **2014**, *43*, 1929-1946.  
15  
16 (46) McNaught, A.D.; Wilkinson, D. Compendium of Chemical Terminology, IUPAC  
17  
18 Recommendation, 2nd ed., Blackwell Sci., Cambridge, **1997**.  
19  
20 (47) Adamson, A.W.; Gast, A.P.: Physical Chemistry of Surface, 6th ed., Wiley, **1997**.  
21  
22 (48) Domańska, U.; Królikowska, M.; Walczak, K. Effect of temperature and composition on  
23  
24 the density, viscosity, surface tension and excess quantities of binary mixtures of 1-ethyl-3-  
25  
26 methylimidazolium tricyanomethanide with thiophene. *Colloids Suf. A: Physicochem. Eng.*  
27  
28 *Asp.* **2013**, *436*, 504-511.  
29  
30 (49) Shereshefsky, J.L. Surface tension of saturated vapors and the equation of Eötvös. *J.*  
31  
32 *Phys. Chem.* **1930**, *35*, 1712-1714.  
33  
34 (50) Guggenheim, E.A. The principle of corresponding states. *J. Chem. Phys.* **1945**, *13*, 253-  
35  
36 261.  
37  
38 (51) Adamson, A.W.; Gast, A.P. Physical Chemistry of Surfaces, 6th ed., Wiley-Interscience,  
39  
40 New York, **1997**.  
41  
42 (52) Renon, H.; Prausnitz, J.M. Local composition in thermodynamic excess functions for  
43  
44 liquid mixtures. *AIChE J.* **14** (1968) 135-144.  
45  
46 (53) Prausnitz, J.M.; Lichtenthaler, R.N.; Azevedo, E.G. *Molecular thermodynamics of*  
47  
48 *fluid-phase equilibria, 2<sup>nd</sup> edition*; Prentice-Hall Inc., Engelwood Cliffs, New Jersey, 1986.  
49  
50  
51  
52  
53  
54  
55  
56  
57  
58  
59  
60

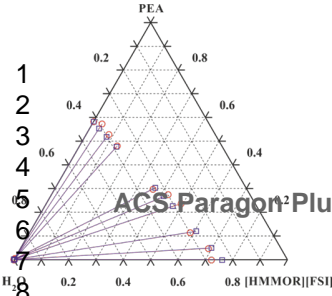
**EXTRACTION**

# EXTRACTION

Page 31 of 38 Journal of Physical Chemistry



2-Phenylethanol



ACS Paragon Plus Environment

